This article has been accepted for publication in IEEE Access. This is the author's version which has not been fully edited and content may change prior to final publication. Citation information: DOI 10.1109/ACCESS.2024.3401569

IEEE Access
Multidisciplinary | Rapid Review | Open Access Journal

Date of publication xxxx 00, 0000, date of current version xxxx 00,0000.

Digital Object Identifier XX/ACCESS.2024.DOI

Multi-Sensor E-Nose based on Online Transfer Learning Trend Predictive Neural Network

PERVİN BULUCU[1], MERT NAKIP[2], and CÜNEYT GÜZELİŞ[3]
[1]Graduate School, Yaşar University, 35100, Izmir, Turkey
[2]Institute of Theoretical and Applied Informatics, Polish Academy of Sciences (PAN), ul. Baltycka 5, 44100, Gliwice, Poland
[3] Department of Electrical and Electronics Engineering, Yaşar University, 35100, Izmir, Turkey

Corresponding author: Mert Nakıp (email: mnakip@iitis.pl)

ABSTRACT Electronic Nose (E-Nose) systems, widely applied across diverse fields, have revolutionized quality control, disease diagnostics, and environmental management through their odor detection and analysis capabilities. The decision and analysis of E-Nose systems often enabled by Machine Learning (ML) models that are trained offline using existing datasets. However, despite their potential, offline training efforts often prove intensive and may still fall short in achieving high generalization ability and specialization for considered application. To address these challenges, this paper introduces the e-rTPNN decision system, which leverages the Recurrent Trend Predictive Neural Network (rTPNN) combined with online transfer learning. The recurrent architecture of the e-rTPNN system effectively captures temporal dependencies and hidden sequential patterns within E-Nose sensor data, enabling accurate estimation of trends and levels. Notably, the system demonstrates the ability to adapt quickly to new data during online operation, requiring only a small offline dataset for initial learning. We evaluate the performance of the e-rTPNN decision system in two domains: beverage quality assessment and medical diagnosis, using publicly available wine quality and Chronic Obstructive Pulmonary Disease (COPD) datasets, respectively. Our evaluation indicates that the proposed e-rTPNN achieves decision accuracy exceeding 97% while maintaining low execution times. Furthermore, comparative analysis against established Machine Learning (ML) models reveals that the e-rTPNN decision system consistently outperforms these models by a significant margin in terms of accuracy.

INDEX TERMS E-Nose, trend prediction, multi-sensor, recurrent trend predictive neural network, online learning,

I. INTRODUCTION

ELECTRONIC Nose (E-Nose) is an analytical device engineered to mimic the mammalian olfactory system through the implementation of a sensor array that responds to a wide range of analytes. They are capable of providing consistent and reproducible results while preventing any potential operator fatigue that can occur during manual odor analysis processes [1]. Their popularity has been growing rapidly ever since the the first design of E-Nose was introduced by Persaud and Dodd [2] in 1982 who presented the idea of an "electronic nose" as a device that utilizes an intelligent array of chemical sensors and pattern recognition techniques to classify odors. E-Noses are low-cost systems that provide rapid response, without requiring laboratory environment or trained professionals.

Following the advancements in sensor technology, materials, software, and microcircuitry, E-Noses have been applied in diverse fields of applications including the food and beverage industry, health care and pharmaceuticals, environmental monitoring, and agriculture [3]. Their capabilities in detecting and analyzing odors have opened up new possibilities for quality control, monitoring, and disease diagnostics, revolutionizing fields ranging from food production to environmental management and healthcare. During the decision making process for various applications, most E-Noses, recently developed, utilize a Machine Learning (ML)-

This work is licensed under a Creative Commons Attribution-NonCommercial-NoDerivatives 4.0 License. For more information, see https://creativecommons.org/licenses/by-nc-nd/4

This article has been accepted for publication in IEEE Access. This is the author's version which has not been fully edited and content may change prior to final publication. Citation information: DOI 10.1109/ACCESS.2024.3401569

based processing algorithms [4]. Those ML algorithms often learn the decision making process based on offline collected data samples exemplifying the targeted application and environment. However, collecting a dataset, which is sufficiently large for obtaining a ML decision system with high generalization ability, is an expensive process that requires extensive experiments. It is also rare to find datasets, available for learning, collected on the exact same E-Nose system and environmental factors. Therefore, one may say that offline training requires intensive effort and can still be insufficient for achieving high generalization ability towards different applications.

In this paper, we present a novel online learning E-Nose decision system based on the Recurrent Trend Predictive Neural Network (rTPNN) [5], [6], which is called e-rTPNN. The proposed e-rTPNN decision system captures both temporal correlations of sensor reading and interrelationships between sensors simultaneously while maximizing the classification accuracy of the E-Nose system. The rTPNN model used in our e-rTPNN decision system is trained in consecutive offline and online stages using transfer learning on model parameters learned using an existing dataset over fixed-length time windows. In offline learning, e-rTPNN first obtains general knowledge by using data obtained from some experiments of the same or similar E-Nose system as the one considered in the online application. In order to address this issue, the proposed e-rTPNN system updates its parameters online via transfer learning. Based on its online learning ability, e-rTPNN can easily and quickly adapt to the characteristics of the application and environment in which it has been newly deployed. In this way, e-rTPNN eliminates the need to collect training data for long periods of time for each new application.

The performance of the new e-rTPNN decision system is evaluated for two different E-Nose applications on wine quality assessment and Chronic Obstructive Pulmonary Disease (COPD) detection using publicly available datasets [7], [8]. We also compare the performance of e-rTPNN with various benchmark models including rTPNN, Long-Short Term Memory (LSTM), Convolutional Neural Network (CNN) and Multi-Layer Perceptron (MLP).

The rest of this paper is organized as follows: Section II reviews the related works focusing on the application areas and deep learning based methods for E-Nose systems. Section III presents the novel online learning e-rTPNN decision system. Section IV, respectively, reviews publicly available E-Nose datasets, evaluates the performance of e-rTPNN and compares that against the well-known ML models as well as the rTPNN model. Finally, Section V concludes this work and presents some open research issues for future work.

II. RELATED WORKS

In recent years, the most common methods for classification and regression problems in E-Nose field have been deep learning based methods. The recent trend of research often uses CNN in order to automatize and learn feature extraction and sensor data fusion in various E-Nose applications [9]–[15]. In [16], CNN was utilized to classify the freshness of 20 different types of food items in three main categories of fruits, vegetables and meats. In [17], a custom CNN structure, based on LeNet-5, was used to effectively classify gases such as CO, CH4, and their mixtures with varying ratios.

On the other hand, Recurrent Neural Network (RNN) models have also been used as a method of choice for E-Nose applications [18]–[20] since they are highly effective and scalable for problems involving sequential data [21]. Differing from other state-of-the-art methods, such as CNN or MLP, the internal memory of RNN allows to extract temporal relationships. This property of RNN is highly desirable for E-Nose applications since sensor readings are often temporally correlated.

In [22], LSTM used with multi-task learning to simultaneously detect gas types and estimate their concentrations. Apart from achieving higher performance results compared to other state-of-the-art methods, it is concluded that two tasks improved each others individual performances. Reference [23] evaluated four RNN models, LSTM, Gated Recurrent Unit (GRU), Bi-directional LSTM (BiLSTM), Bi-directional GRU (BiGRU), for high-precision monitoring of ethanol and glucose during simultaneous saccharification and fermentation of cassava. Authors used commercially available PEN3 E-Nose for gas measurements. BiLSTM achived 98% coefficient of predictive determination for ethanol while GRU obtained 99% for glucose, proving the eligibility of RNN models for E-Nose applications. Reference [24] developed GRU based auto-encoder (GRU-AE) model combined with ensemble pruning model to extract temporal and high-dimensional features for lung cancer detection, where GRU-AE achieved 94.22% sensitivity and 93.55% accuracy.

Some research [25]–[30] combined LSTM with CNN, creating hybrid architectures. Reference [25] proposed a novel deep learning model with Convolutional LSTM (ConvLSTM) layers to predict odor descriptor ratings (e.g. garlic, fish, burnt etc.). ConvLSTM layers learn spatiotemporal features from the sensor data. They extract temporal characteristics of the signals while simultaneously utilizing the interdependencies between sensors. The performance of this model is compared with state-of-the-art models such as CNN and LSTM. It was concluded that utilizing the spatiotemporal features of the sensor data is more effective than utilizing the spatial or temporal features separately. A hybrid deep learning method (H-CRNN) was proposed for early detection of low concentration carbon-monoxide (CO) gas [26]. The convolution layer captures short-term dependencies from sensor data, while the recurrent layer explores long-term dependencies. The results showed that, especially with higher prediction horizons, H-CRNN Proposed model combined with a gated attention mechanism performed significantly better compared with recurrent models. Reference [27] tested several models including CNN, CNN-LSTM, LSTM, GRU, CNN-GRU for asthma detection problem.

E-Nose technology holds significant promise for vari-

This work is licensed under a Creative Commons Attribution-NonCommercial-NoDerivatives 4.0 License. For more information, see https://creativecommons.org/licenses/by-nc-nd/4

This article has been accepted for publication in IEEE Access. This is the author's version which has not been fully edited and content may change prior to final publication. Citation information: DOI 10.1109/ACCESS.2024.3401569

ous applications, ranging from industrial quality control to medical diagnostics. Leveraging deep learning techniques such as CNNs and RNNs, researchers have achieved remarkable results in feature extraction, sensor data fusion, and temporal relationship extraction. This interdisciplinary approach has enabled E-Noses to provide real-time results with on-site measurements, contributing to reducing food waste, decreasing quality control costs, and offering non-invasive alternatives for disease diagnosis and monitoring in the medical field. By analyzing breath and urine samples, E-Noses offer potential solutions for early disease detection, bio-marker tracking, and infection identification, thus improving patient care and overall public health. As the food and beverage industry is one of the most important beneficiaries of high-tech E-Noses, recent research utilized an E-Nose for spoilage detection [31], quality assessment [16], shelf-life investigation [32], adulteration detection [33], [34], contamination detection, flavor profiling, mimicking sensory analysis [35], tracking the fermentation process [36]. Extensive research has been conducted on a wide variety of food products, such as mushrooms, coffee, tea, meat, maize, wine, and beer. Utilization of E-Noses for the food and beverage industry can help manufacturers reduce food waste and decrease the cost of quality control. In addition, E-Noses are capable of decreasing the time consumed during the quality control process by providing real-time results with on-site measurements. These measurements are possible due to the nature of the device, which does not require a special sampling process.

E-Noses were also proved to be very useful for medical field, especially for non-invasive diagnostic solutions. The application areas include disease diagnostics, early detection, disease progression monitoring, biomarker tracking, identification of infections, quality control etc. Human exhaled breath contains over 3000 volatile organic compounds [37]. By studying breath signature E-Noses can be predictive of numerous respiratory and systematic diseases. There is extensive research for the non-invasive diagnosis of pulmonary diseases such as; COPD, Covid-19, lung cancer, cystic fibrosis from the exhaled breath [38]–[40]. Also, by analyzing blood glucose levels, E-Noses can be utilized as non-invasive diagnostic tools for diabetes. Additionally, E-Noses have been proposed for identifying VOCs in the urine of women with cervical cancer [41].

III. THE E-RTPNN DECISION SYSTEM WITH ONLINE TRANSFER LEARNING

In this section, we present the proposed e-rTPNN decision system. To this end, we describe the architectural design of the rTPNN, and we detail its online transfer learning algorithm. The e-rTPNN decision system, given in Figure 1, process the data read through an array of N sensors using the rTPNN model with online transfer learning. We let x_n^k denote the data reading of sensor n sampled at discrete time k.

As presented in Figure 1, e-rTPNN calculates the probability y_M of each class M based on the current and previous sensor readings $\{x_n^k\}_{n\in\{1,\dots,N\}}$ and $\{x_n^{k-1}\}_{n\in\{1,\dots,N\}}$ at each sampling time k. To this end, the e-rTPNN decision system is comprised of rTPNN specific layer and fully connected layers along with the online transfer learning.

A. RTPNN LAYER: EXPECTED LEVEL AND TEMPORAL TREND

rTPNN layer, which is the first layer in our e-rTPNN system, is used to extract the temporal features – trend t_n^k and level l_n^k – for the reading of each sensor n.

rTPNN [6] is capable of performing classification based on multi-sensor time series data while predicting trends and levels of the data simultaneously. Diverging from established methods that only use the present data in a sequential manner, the recursive structure of rTPNN allows for predictions based on the progression of previous data in addition to the current sensor readings. This property allows rTPNN to be resilient against sudden fluctuations of sensor data that may be caused due to hardware malfunction, noise, or data processing errors in E-Nose systems. As shown in earlier applications of rTPNN for fire detection [6] and renewable energy management [42], rTPNN's internal structure can capture the patterns inherent in time series data, hence reducing the error in the output and effectively increasing the predictive capabilities of the network.

The rTPNN layer is comprised of two units, Trend Predictor and Level Predictor, which are detailed in Figure 2, for each sensor n. These units take the current and previous sensor readings x_n^k and x_n^{k-1} and calculate temporal trend t_n^k and expected level l_n^k. The output of the rTPNN layer consists of N channels, each of which is a vector of $[x_n^k, t_n^k, l_n^k]^T$.

1) Trend Predictor

Trend predictor module calculates the trend of the sensor data

$$t_n^k = \alpha_n^1(x_n^k - x_n^{k-1}) + \alpha_n^2 t_n^{k-1} \tag{1}$$

The architecture of the trend predictor module is a linear recurrent neuron. As given in (1), the trend predictor calculates the trend t_n^k based on a current sensor reading x_n^k, the previous sensor reading x_n^{k-1} and the value of trend t_n^{k-1} previously calculated. The parameters α_n^1 and α_n^2 are learned during the training using an offline collected dataset.

2) Level Predictor

The level predictor module computes the expected level l_n^k based on the current sensor reading x_n^k and previously predicted level l_n^{k-1}:

$$l_n^k = \beta_n^1 x_n^k + \beta_n^2 l_n^{k-1} \tag{2}$$

The architecture of the level predictor module is a linear recurrent neuron, as shown in Figure 2. The parameters β_n^1 and β_n^2 are the weights of the recurrent neuron and are learned by the recurrent neuron during training.

This work is licensed under a Creative Commons Attribution-NonCommercial-NoDerivatives 4.0 License. For more information, see https://creativecommons.org/licenses/by-nc-nd/4

This article has been accepted for publication in IEEE Access. This is the author's version which has not been fully edited and content may change prior to final publication. Citation information: DOI 10.1109/ACCESS.2024.3401569

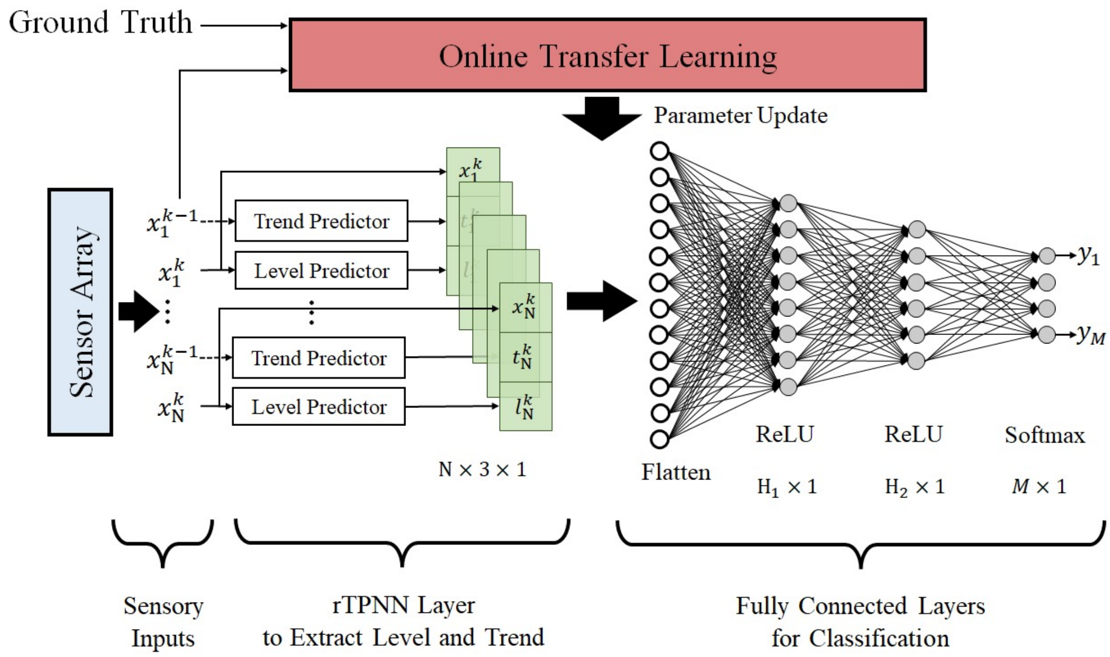

FIGURE 1: The architectural design of the proposed e-rTPNN decision system, which is based on the rTPNN model with online transfer learning

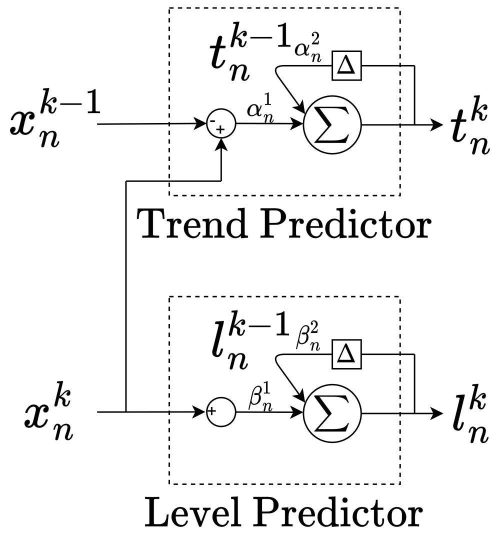

FIGURE 2: Trend and Level Predictor units of the rTPNN layer for a sensor n

B. FULLY CONNECTED LAYERS: MULTI-CLASS CLASSIFICATION

The final layers of the rTPNN model are the three fully connected layers used for the classification task. Two of these layers have H_1 and H_2 neurons, respectively, each of which utilizes the ReLU activation function. The last fully connected layer is the output layer with M neurons with a softmax activation function. Here M is equal to the number of output classes for each dataset. The computation of H_1 and H_2 are given in (3) and (4):

$$H_2 = \mathcal{F}(2M) \tag{3}$$
$$H_1 = 2\,H_2 \tag{4}$$

Where $\mathcal{F}(\cdot)$ is the function that calculates the nearest power of two of its input.

The forward pass of these layers are simply:

$$Z_1^k = \mathrm{ReLU}(\mathbf{W}_1\, Z_0^k) + B_1, \tag{5}$$
$$Z_2^k = \mathrm{ReLU}(\mathbf{W}_2\, Z_1^k) + B_1, \tag{6}$$
$$Y^k = \mathrm{softmax}(\mathbf{W}_3\, Z_2^k) \tag{7}$$

where $\mathbf{W}_h$ is the input weights matrix, B_h is the vector of biases, and Z_h^k is the output of hidden layer h. In particular, $Z_0^k = \left[t_n^k, l_n^k, x_n^k : n \in \{1, \dots, N\}\right]$. In addition, Y^k is the output vector of the rTPNN model, and the softmax$(\cdot)$ activation function is defined as

$$\mathrm{softmax}(a_i) = \frac{e^{a_i}}{\sum_{j=1}^{M} e^{a_j}}, \quad \text{for } i = 1, 2, \dots, M. \tag{8}$$

C. ONLINE TRANSFER LEARNING

We now present the operation of the e-rTPNN decision system, which is presented in Algorithm 1, focusing on its online learning.

As shown on lines 1-4 of Algorithm 1, the rTPNN model is first trained offline prior to the online operation using the available dataset. To this end, on line 1, the input data $X_{\text{off}}^{\text{train}}$ and the corresponding desired output $D_{\text{off}}^{\text{train}}$ are obtained from the offline dataset. Then, on lines 2 and 3, the set of rTPNN parameters, denoted by $\mathcal{P}$, is initialized randomly from normal distribution and updated until the training error

This work is licensed under a Creative Commons Attribution-NonCommercial-NoDerivatives 4.0 License. For more information, see https://creativecommons.org/licenses/by-nc-nd/4

This article has been accepted for publication in IEEE Access. This is the author's version which has not been fully edited and content may change prior to final publication. Citation information: DOI 10.1109/ACCESS.2024.3401569

Algorithm 1 The e-rTPNN decision system with online transfer learning

1: $(X_{\text{off}}^{\text{train}}, D_{\text{off}}^{\text{train}}) \leftarrow$ **get_offline_data**();
2: $\mathcal{P} \leftarrow$ **initialize**();
3: $\mathcal{P} \leftarrow$ **rTPNN_fit**($\mathcal{P}, X_{\text{off}}^{\text{train}}, D_{\text{off}}^{\text{train}}$);
4: $X^0 \leftarrow$ **read_sensor_data**();
5:
6: $X_{\text{on}}^{\text{train}} = []$;
7: **for** $(k = 1, k{+}{+}, k < \infty)$ **do**
8: $\quad X^k \leftarrow$ **read_sensor_data**();
9: $\quad X_{\text{on}}^{\text{train}} \leftarrow [X_{\text{on}}^{\text{train}}, X^k]$;
10: $\quad Y^k \leftarrow$ **rTPNN_predict**($\mathcal{P}, X^k, X^{k-1}$);
11:
12: $\quad$ **if** $(k \mod K) == 0$ **then**
13: $\quad\quad D_{\text{on}}^{\text{train}} \leftarrow$ **get_ground_truth**(k);
14: $\quad\quad \mathcal{P} \leftarrow$ **rTPNN_fit**($\mathcal{P}, X_{\text{on}}^{\text{train}}, D_{\text{on}}^{\text{train}}$);
15: $\quad\quad X_{\text{on}}^{\text{train}} = []$;
16: $\quad$ **end if**
17:
18: **end for**

does not improve for 3 successive epochs. The vector of initial sensor readings, denoted by X^0, is then obtained for $k = 0$ on line 4, where $X^k = [x_1^k, \ldots, x_N^k]$.

The online operation of the e-rTPNN decision system is given from line 7 to line 18. Prior to the online operation of the For each discrete time k, first, the vector current sensor readings, X^k, is obtained on line 8 and added into the list of inputs, denoted by $X_{\text{on}}^{\text{train}}$, to be used for online learning on the following line 9. Subsequently, based on X^k and the most recent rTPNN parameters $\mathcal{P}$, the output vector Y^k is calculated through equations (5)-(7).

If the current time window k is a multiple of the online training period K (line 12), the rTPNN parameters are updated between lines 13 and 15. The rTPNN parameters are updated using supervised learning with back-propagation through time. Therefore, on line 13, the list of desired output vectors, denoted by $D_{\text{on}}^{\text{train}}$, corresponding to the list of inputs $X_{\text{on}}^{\text{train}}$, i.e. the labeled training data, is provided. Using $X_{\text{on}}^{\text{train}}$ and $D_{\text{on}}^{\text{train}}$, the rTPNN parameters are updated on line 14. After the training is completed, $X_{\text{on}}^{\text{train}}$ is cleared on line 15.

IV. RESULTS

In this section, we present the performance of the proposed e-rTPNN model in comparison with original rTPNN model when applied to the publicly available E-Nose datasets, which shall be presented in Section IV-A. To this end, we first analyze the datasets used to obtain performance evaluation results. Then, we evaluate the performance of the models in terms of accuracy, recall, F1 score, specificity and Matthew Correlation Coefficient (MCC). We present the benefits of the online learning approach compared to the standard offline learning.

Furthermore, we conduct a comparative analysis with other state-of-the-art machine learning models. Specifically, we evaluate the effectiveness of e-rTPNN alongside LSTM, MLP, and CNN when applied to the same problem. We also present the structure of these models and the details of their parameter tuning in Section IV-D1

A. DATASETS AND THEIR ANALYSIS

We evaluate the performance of the proposed e-rTPNN using the sensor data provided by two online available datasets for wine spoilage detection [7] and COPD detection [8].

1) Wine Spoilage Detection

A time series dataset is provided in [7] for a wine quality detection application that specifically focuses on spoilage thresholds. The dataset consists of 235 recorded measurements of wines, which are categorized into three groups: high quality (HQ), average quality (AQ), and low quality (LQ). In addition to these groups, the dataset includes 65 recorded measurements for ethanol. Each recorded measurement file is comprised of 3330 samples corresponding to 180 seconds. The data was collected using an E-Nose system that utilizes 6 MOS gas sensors, with two sensors each for:

- MQ3: methane, hexane, LPG, CO, alcohol, and benzene
- MQ4: methane and natural gas
- MQ6: propane, LPG, and iso-butane

Although some samples also included measurements of relative humidity and temperature, the present paper will only consider the outputs of the gas sensors due to missing data samples of relative humidity and temperature. Original sensor data was inverted to transform kilo-ohm units to Siemens unit since Siemens data increases-decreases in proportion with the gas concentration in the chamber.

Figure 3 shows the transformed sensor readings for each class.

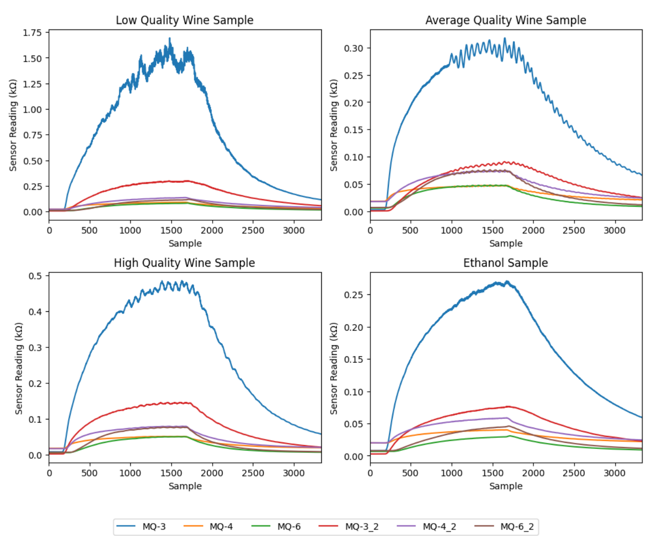

FIGURE 3: Sensor outputs for a sample wine bottles of each class.

This work is licensed under a Creative Commons Attribution-NonCommercial-NoDerivatives 4.0 License. For more information, see https://creativecommons.org/licenses/by-nc-nd/4

This article has been accepted for publication in IEEE Access. This is the author's version which has not been fully edited and
content may change prior to final publication. Citation information: DOI 10.1109/ACCESS.2024.3401569

2) COPD Detection

Chronic Obstructive Pulmonary Disease dataset [8] is obtained on exhaled breath of a group of patients by using an array of MOS sensors:

- SP-3: Alcholol, solvent
- MQ-3: Methane, LPG, hexane, alcohol, CO, benzene
- MQ-135: Ammonia, carbon dioxide, NOx, benzene, alcohol, smoke
- MQ-137: Ammonia
- MQ-138: Toluene, acetone, alcohol, methanol
- TGS 800: CO, methane, isobutane, hydrogen and ethanol.
- TGS 813: Combustible gases (i.e. methane, propane, butane)
- TGS 822: Ethanol, Solvent Vapors

The dataset contains samples collected from 20 people affected by COPD, 4 smokers, and 10 healthy control individuals. In addition, there are 10 files collected only for air. Sensor reading measurements for each class of COPD, smoker, healthy individual, and air are given in Figure 4.

For this dataset, due to unbalanced number of samples where COPD class has significantly more samples in comparison with other classes, we opted out for binary classification in order to detect whether a sample belongs to a COPD patient or not.

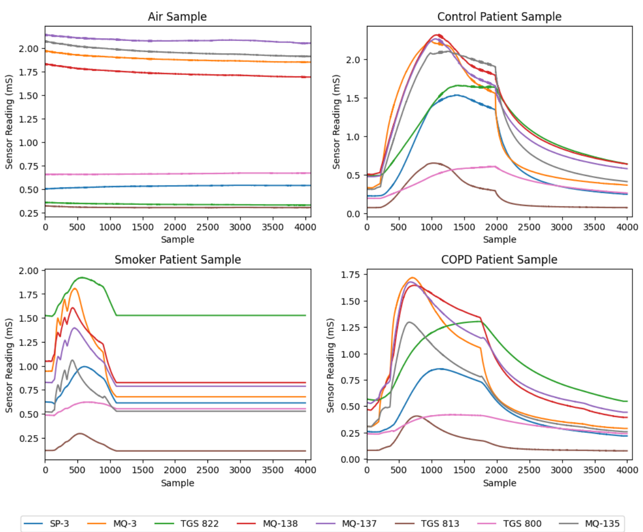

FIGURE 4: Exhaled breath samples acquired with the E-Nose device for AIR, COPD, Smoker and Control (healthy)

B. PERFORMANCE METRICS

In order to reduce possible bias that can occur due to random split of train/test datasets and test the generalization abilities and robustness of the networks, 5-fold cross-validation was employed to assess the performances of proposed e-rTPNN and compared methods.

Since models were tested on multi-class classification problems, performance criteria will be presented for each class, as well as the overall test accuracy. We present test accuracy, recall, specificity, F1 scores and Matthews Correlation Coefficient (MCC) for each class. All of the results were obtained by averaging the results of 5 trainings of 5-fold cross validation.

Accuracy is computed by taking the percentage correctly classified samples to all the instances in a dataset. It is calculated as $Accuracy = \frac{TP+TN}{TP+FP+TN+FN}$, where TP= True positive, TN= True negative, FP= False positive, FN= False negative. For our problem, we calculated binary accuracy values for each class, by treating every sample belonging to that class as a positive sample and all others as negative samples.

Specificity, or the True Negative Rate, is the measure of a model's ability to correctly identify negative instances and calculated as $\frac{\text{TN}}{\text{TN+FP}}$. Recall, also known as Sensitivity or True Positive Rate, evaluates the capability of the model to correctly identify positive instances and is calculated as: $\frac{TP}{TP+FN}$ which is the ration of detected positive samples to all positive samples. The higher the recall value, the more positive samples were detected.

F1 score is the harmonic mean of precision and recall and is calculated as $\frac{2\times(\text{Precision}\times\text{Recall})}{\text{Precision}+\text{Recall}}$, where Precision is computed as $\frac{\text{TP}}{\text{TP+FP}}$.

MCC is a highly reliable evaluation metric as it takes into account all four of the confusion matrix elements and produces high scores only if the prediction obtained good results in all of these categories. MCC is calculated as $\frac{(TP\cdot TN)-(FP\cdot FN)}{\sqrt{(TP+FP)\cdot(TP+FN)\cdot(TN+FP)\cdot(TN+FN)}}$.

C. ONLINE TRANSFER LEARNING VS OFFLINE LEARNING

1) Class Accuracy

Table 1 presents average accuracy results over 5 folds and standard deviations for all classes and overall accuracy results for whole datasets.

TABLE 1: Test accuracy comparison of online e-rTPNN and offline rTPNN

Dataset	Class	Models	
		e-rTPNN	rTPNN
Wine	LQ	0.9808 ± 0.0013	0.9460 ± 0.0230
	AQ	0.9754 ± 0.0018	0.9868 ± 0.0104
	HQ	0.9843 ± 0.0056	0.9498 ± 0.0171
	Ethanol	0.9844 ± 0.0019	0.9741 ± 0.0071
	Overall Accuracy	0.9625 ± 0.0028	0.9284 ± 0.0230
COPD	Overall Accuracy	0.9693 ± 0.0500	0.9400 ± 0.0221

Looking at the Table 1, we observe that online learning approach increased the performance of the standard e-rTPNN in a significant way. Not only the classification accuracy increased for almost all classes, the overall accuracy increased from 92 % to 96 % for the wine dataset, and from 94 % to 97

This work is licensed under a Creative Commons Attribution-NonCommercial-NoDerivatives 4.0 License. For more information, see https://creativecommons.org/licenses/by-nc-nd/4

This article has been accepted for publication in IEEE Access. This is the author's version which has not been fully edited and content may change prior to final publication. Citation information: DOI 10.1109/ACCESS.2024.3401569

TABLE 2: Recall, Specificity, F1 Score and MCC comparison of e-rTPNN and rTPNN

Dataset	Class Label	Model	Recall	Specificity	F1 Score	MCC
Wine	LQ	e-rTPNN	0.9539	0.9882	0.9555	0.9433
		rTPNN	0.8645	0.9697	0.8727	0.8406
	AQ	e-rTPNN	0.9765	0.9736	0.9734	0.9499
		rTPNN	0.9892	0.9842	0.9860	0.9736
	HQ	e-rTPNN	0.9439	0.9904	0.9454	0.9361
		rTPNN	0.8671	0.9643	0.8250	0.7986
	Ethanol	e-rTPNN	0.9451	0.9921	0.9525	0.9431
		rTPNN	0.9006	0.9890	0.9210	0.9058
COPD	Overall	e-rTPNN	0.9896	0.9455	0.9726	0.9416
		rTPNN	0.9634	0.9226	0.9365	0.8825

% for the COPD detection dataset. Furthermore, we can see that standard deviation values are much lower for the online method, suggesting a more consistently high performance.

In online learning, algorithm goes over every test sample one-by-one. We can observe the effect of this method in Fig 5 that shows a random part of true labels and corresponding predictions made by the online model for a wine sample. When observing the figure we can see where accuracy drops at beginning of each new sample, and then fixes itself at the next window. Every sample has 3300 data points and we can see a slight drop of accuracy at the beginning of new samples only to be quickly fixed by the algorithm.

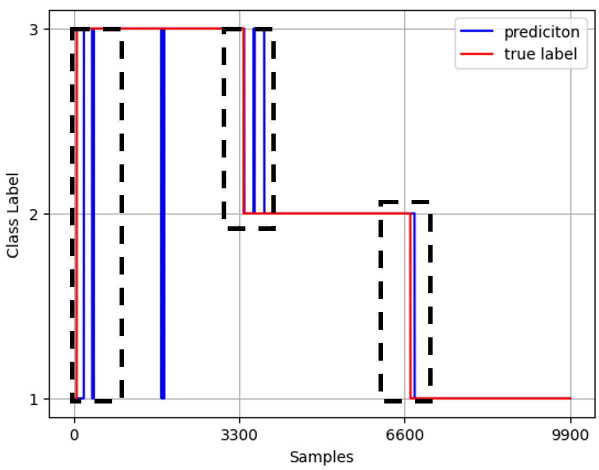

FIGURE 5: Model predictions vs true labels during online learning for three samples. Marked areas show wrong predictions at the start of new samples and the quick recovery of the algorithm.

2) Recall, Specificity, F1 Score and MCC

We present the performance results of e-rTPNN and rTPNN in Table 2. In our case, multi-class classification, we measure the model's ability to detect the positive samples for each class. Looking at the Table 2, we see that recall metric increased for every class, except the average quality wine class, which was already very high.

Table 2 shows that specificity was very high for offline e-rTPNN to begin with. However there is still a slight increase in performance due to the online learning approach. F1 score, that presents the balance between recall and precision significantly increased after the online learning approach. This shows that online learning increases both recall and precision. Especially for high quality wine dataset samples, F1-score of the offline method increased from a low 82% to a very high 94%.

Table 2 present a steep increase in MCC performance. For high quality wine samples, MCC increased from 79% to 93% and for the COPD dataset MCC went from 88% to 94%.

The results of this section show that there is a very clear advantage of using online transfer learning based approach. Apart from its ability to adapt to new information, this method increased all of the performance evaluation metrics.

D. E-RTPNN VS STATE-OF-THE-ART METHODS

After comparing the online transfer learning based e-rTPNN to the offline model, we also compare our models to the stare-of-art classification methods, commonly used for E-Nose applications.

1) Methods Used for Comparison

In this section, we briefly explain the structures of these models.

LSTM model is often applied to the same problems, in order to compare the performance of the proposed methods to a state-of-the-art RNN structure. We construct an LSTM network with a 64 LSTM cells and the same fully connected structure of the e-rTPNN model with H_1, H_2 and M neurons to keep the model architectures similar.

CNN model is constructed to observe the performance of a convolutional structure without the trend and level information of the recurrent model. Similar to the LSTM model, to keep the structures similar, CNN model structure included two 1D convolutional layers with F_T and F_R neurons and the fully connected layers with H_1, H_2, M neurons. Here F_T

This work is licensed under a Creative Commons Attribution-NonCommercial-NoDerivatives 4.0 License. For more information, see https://creativecommons.org/licenses/by-nc-nd/4

This article has been accepted for publication in IEEE Access. This is the author's version which has not been fully edited and
content may change prior to final publication. Citation information: DOI 10.1109/ACCESS.2024.3401569

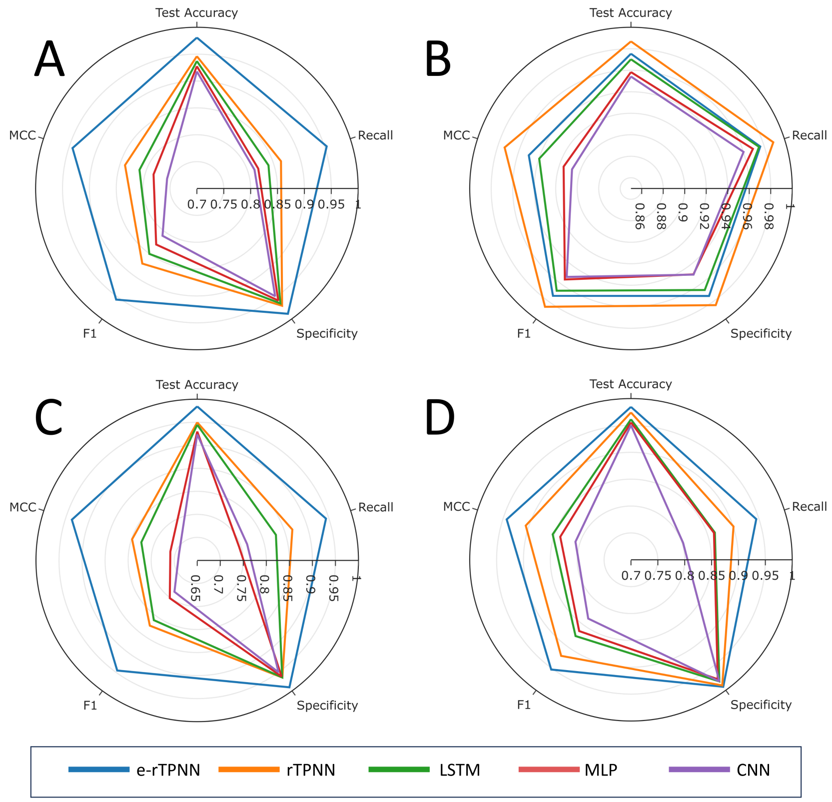

FIGURE 6: Star diagrams for performance results on wine dataset for the classes A: Low Quality, B: Average Quality, C: High Quality, D: Ethanol

and F_R are calculated as:

$$F_T = \mathcal{F}\left(\sqrt{\frac{8\,H_1}{N/2}}\right) \tag{9}$$

$$F_R = F_T \tag{10}$$

where $\mathcal{F}$ is the function that calculates power of two value that is nearest to its input and N is the number of sensors.

MLP model is applied to observe the network performance without the trend and level data as well as the high level features extracted by the convolutional layers. Model was constructed with the fully connected structure of the e-rTPNN (H_1, H_2, M neurons).

All methods used ReLU activation function for hidden layers and softmax activation function for the final layer.

2) Performance Results on Wine Dataset

Fig 6 presents the star diagram with the performance results of all methods applied to wine dataset. From the figure, we can see that except the average quality class where all models achieved satisfactory results, there are drastic performance differences between rTPNN and state-of-the-art methods. On top of that e-rTPNN managed to take this a step further, surpassing the performance of even the rTPNN, which was already higher compared to the other models.

We see that, high quality class was challenging for most of methods. Even rTPNN has relatively low scores. e-rTPNN on the other hand, manages to improve on all evaluation metrics, almost reaching the perfect score. The overall test accuracy results for e-rTPNN, rTPNN, LSTM, CNN and MLP are respectively 0.9625, 0.9284, 0.9066, 0.873 and 0.8857.

3) Performance Results on COPD Dataset

The overall test accuracy results for e-rTPNN, rTPNN, LSTM, CNN and MLP are 0.9693, 0.9400, 0.9314, 0.9539 and 0.9149 respectively. Star diagram with the performance results of all methods applied to the COPD dataset are given in Fig 7. From the figure, we see that e-rTPNN achieved the highest performance results. In contrast with the wine dataset, MLP performed higher that the LSTM model. With that, we can deduce that the online learning approach of the e-rTPNN manages to overcome the issues these models faced, reaching almost 97 % test accuracy.

One observation that needs to be highlighted, is the low performance of the CNN model. CNN is a widely utilized method for many classification algorithms, including E-Nose applications. However, our results show that e-rTPNN significantly outperform the CNN model. This indicates that proposed model structure is more suitable for these type of problems, where time series data is being utilized.

E. COMPUTATION TIME MEASUREMENTS

Training and testing times for rTPNN, LSTM, CNN and MLP are given in Figure 8. Note that all experiments were

This work is licensed under a Creative Commons Attribution-NonCommercial-NoDerivatives 4.0 License. For more information, see https://creativecommons.org/licenses/by-nc-nd/4

This article has been accepted for publication in IEEE Access. This is the author's version which has not been fully edited and
content may change prior to final publication. Citation information: DOI 10.1109/ACCESS.2024.3401569

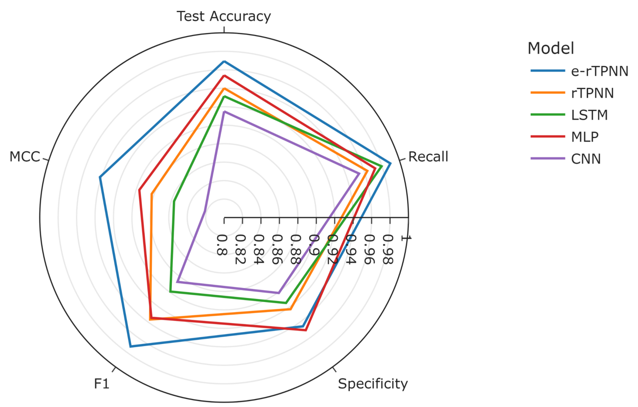

FIGURE 7: Star diagram for performance results on COPD dataset

constructed with Python's Keras library and run on Google Colab using Central Processing Unit (CPU). Google Colab utilizes 2.20GHz Intel®Xeon®CPU.

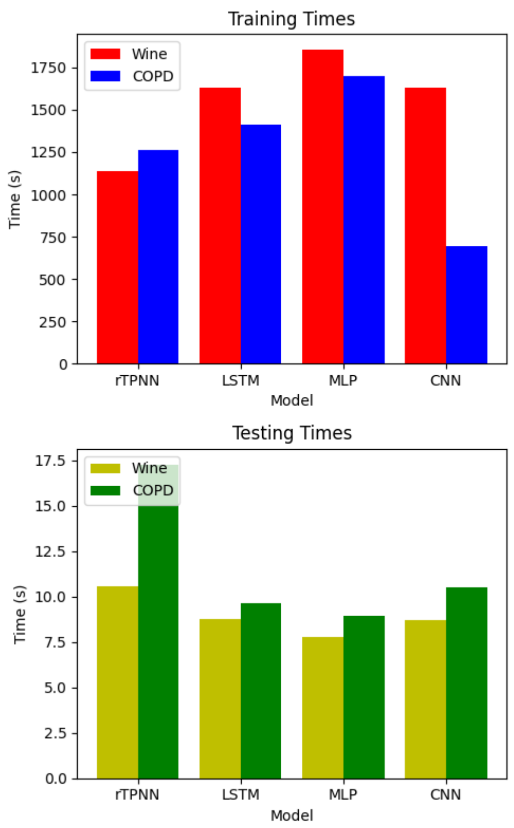

FIGURE 8: Training and testing times for models

Training times were computed until the model reaches the best performance results. From the figure, we can see that rTPNN reached best weights a lot faster when compared to other models. The short training time of the CNN on COPD model, was due to models inability to further increase its performance. Since e-rTPNN with online transfer goes through every test sample one at a time with the batch size of 1, the learning times differ from the offline counterparts.

V. CONCLUSION

In this paper, for E-Nose applications, we have developed e-rTPNN decision system which learns from both offline available dataset(s) and online self-collected sensory data. The e-rTPNN system enables capturing temporal dependencies and hidden sequential patterns due to its recurrent structure that estimate the trend and level of the time series data. Moreover, the developed online transfer learning approach of e-rTPNN, consisting of two consecutive stages, improves classification performance by learning from both existing offline datasets and sensor readings collected online in fixed-length time windows. Based on its online transfer learning approach, the e-rTPNN decision system can quickly adapt to new environments and data obtained from these environments, eliminating the need for collecting new training data.

Furthermore, we have tested the performance of the e-rTPNN model on publicly available wine quality assessment and COPD detection E-Nose datasets. We compare the performance of the proposed method with the state-of-the-art CNN, MLP, and LSTM models. In order to test the generalization abilities of these models and prevent skewed results due to the selection of train-test datasets all training was performed with 5-fold cross-validation. The test results showed that the proposed e-rTPNN system achieves above 97% accuracy with considerably low training and execution times. In addition, for the majority of experiments, e-rTPNN outperforms the compared models by a significantly large performance margin (varying from 1% to 5%).

As this paper developed the e-rTPNN decision system and evaluated its capabilities for E-Nose applications, future work shall implement and test the e-rTPNN system for real-time experiments on an actual E-Nose hardware setup.

ACKNOWLEDGEMENT

The support of the TUBITAK 2244 under Grant Agreement No. 119C171 is gratefully acknowledged.

REFERENCES

[1] A. D. Wilson and M. Baietto, "Applications and advances in electronic-nose technologies," *Sensors*, vol. 9, no. 7, pp. 5099–5148, jul 2009.
[2] K. Persaud and G. Dodd, "Analysis of discrimination mechanisms in the mammalian olfactory system using a model nose," *Nature*, vol. 299, no. 5881, pp. 352–355, 1982.
[3] A. D. Wilson, "Diverse applications of electronic-nose technologies in agriculture and forestry," *Sensors (Switzerland)*, vol. 13, no. 2, pp. 2295–2348, 2013.
[4] E. A. Baldwin, J. Bai, A. Plotto, and S. Dea, "Electronic noses and tongues: Applications for the food and pharmaceutical industries," *Sensors*, vol. 11, no. 5, pp. 4744–4766, 2011.
[5] M. Nakıp and C. Güzeliş, "Multi-sensor fire detector based on trend predictive neural network," in *2019 11th International Conference on Electrical and Electronics Engineering (ELECO)*. IEEE, 2019, pp. 600–604.
[6] M. Nakip, C. Guzelis, and O. Yildiz, "Recurrent Trend Predictive Neural Network for Multi-Sensor Fire Detection," *IEEE Access*, vol. 9, pp. 84 204–84 216, 2021.
[7] J. C. Rodriguez Gamboa, E. S. Albarracin E., A. J. da Silva, and T. A. Tiago, "Electronic nose dataset for detection of wine spoilage thresholds," *Data in Brief*, vol. 25, p. 104202, 2019. [Online]. Available: https://doi.org/10.1016/j.dib.2019.104202

This work is licensed under a Creative Commons Attribution-NonCommercial-NoDerivatives 4.0 License. For more information, see https://creativecommons.org/licenses/by-nc-nd/4

This article has been accepted for publication in IEEE Access. This is the author's version which has not been fully edited and
content may change prior to final publication. Citation information: DOI 10.1109/ACCESS.2024.3401569

[8] C. M. D. Acevedo, C. A. C. Vasquez, and J. K. C. Gómez, "Electronic nose dataset for COPD detection from smokers and healthy people through exhaled breath analysis," *Data in Brief*, vol. 35, pp. 4–9, 2021.
[9] S. Wang, Q. Zhang, C. Liu, Z. Wang, J. Gao, X. Yang, and Y. Lan, "Synergetic application of an E-tongue, E-nose and E-eye combined with CNN models and an attention mechanism to detect the origin of black pepper," *Sensors and Actuators A: Physical*, vol. 357, no. March, p. 114417, 2023. [Online]. Available: https://doi.org/10.1016/j.sna.2023.114417
[10] Y. Shi, F. Gong, M. Wang, J. Liu, Y. Wu, and H. Men, "A deep feature mining method of electronic nose sensor data for identification identifying beer olfactory information," *Journal of Food Engineering*, vol. 263, no. February, pp. 437–445, 2019. [Online]. Available: https://doi.org/10.1016/j.jfoodeng.2019.07.023
[11] O. Attallah, "Multitask Deep Learning-Based Pipeline for Gas Leakage Detection via E-Nose and Thermal Imaging Multimodal Fusion," *chemosensors*, vol. 11, no. 364, 2023.
[12] S. Zhang, Y. Cheng, D. Luo, J. He, A. K. Wong, and K. Hung, "Channel Attention Convolutional Neural Network for Chinese Baijiu Detection with E-Nose," *IEEE Sensors Journal*, vol. 21, no. 14, pp. 16 170–16 182, 2021.
[13] Z. Hui and A. Lu, "A deep learning method combined with an electronic nose for gas information identification of soybean from different origins," *Chemometrics and Intelligent Laboratory Systems*, vol. 240, no. June, 2023.
[14] J. C. Rodriguez Gamboa, A. J. da Silva, I. C. Ismael, E. S. Albarracin E., and C. M. Duran A., "Validation of the rapid detection approach for enhancing the electronic nose systems performance, using different deep learning models and support vector machines," *Sensors and Actuators, B: Chemical*, vol. 327, no. May 2020, p. 128921, 2021. [Online]. Available: https://doi.org/10.1016/j.snb.2020.128921
[15] D. Wu, D. Luo, K. Y. Wong, and K. Hung, "POP-CNN: Predicting Odor Pleasantness with Convolutional Neural Network," *IEEE Sensors Journal*, vol. 19, no. 23, pp. 11 337–11 345, 2019.
[16] X. Ren, Y. Wang, Y. Huang, M. Mustafa, D. Sun, F. Xue, D. Chen, L. Xu, and F. Wu, "A CNN-based E-nose using Time Series Features for Food Freshness Classification," *IEEE Sensors Journal*, vol. 23, no. 6, pp. 6027–6038, 2023.
[17] G. Wei, G. Li, J. Zhao, and A. He, "Development of a LeNet-5 gas identification CNN structure for electronic noses," *Sensors (Switzerland)*, vol. 19, no. 1, 2019.
[18] Q. Wang, H. Qi, and F. Liu, "Time series prediction of e-nose sensor drift based on deep recurrent neural network," *Chinese Control Conference, CCC*, vol. 2019-July, pp. 3479–3484, 2019.
[19] Y. Zou and J. Lv, "Using recurrent neural network to optimize electronic nose system with dimensionality reduction," *Electronics*, vol. 9, no. 12, 2020. [Online]. Available: https://www.mdpi.com/2079-9292/9/12/2205
[20] D. R. Wijaya, R. Sarno, and E. Zulaika, "DWTLSTM for electronic nose signal processing in beef quality monitoring," *Sensors and Actuators, B: Chemical*, vol. 326, no. May 2019, p. 128931, 2021. [Online]. Available: https://doi.org/10.1016/j.snb.2020.128931
[21] J. Torres-tello, G. S. Member, and A. V. Guaman, "Improving the Detection of Explosives in a MOX Chemical Sensors Array With LSTM Networks," vol. 20, no. 23, pp. 14 302–14 309, 2020.
[22] H. Liu, Q. Li, and Y. Gu, "A multi-task learning framework for gas detection and concentration estimation," *Neurocomputing*, vol. 416, pp. 28–37, 2020. [Online]. Available: https://www.sciencedirect.com/science/article/pii/S0925231220301028
[23] B. Wang, J. Deng, H. Jiang, and Q. Chen, "Electronic nose signals-based deep learning models to realize high-precision monitoring of simultaneous saccharification and fermentation of cassava," *Microchemical Journal*, vol. 182, no. June, p. 107929, 2022. [Online]. Available: https://doi.org/10.1016/j.microc.2022.107929
[24] B. Lu, L. Fu, B. Nie, Z. Peng, and H. Liu, "A novel framework with high diagnostic sensitivity for lung cancer detection by electronic nose," *Sensors*, vol. 19, no. 23, 2019. [Online]. Available: https://www.mdpi.com/1424-8220/19/23/5333
[25] J. Guo, Y. Cheng, D. Luo, K.-y. Wong, K. Hung, and X. Li, "ODRP : A Deep Learning Framework for Odor Descriptor Rating Prediction Using Electronic Nose," *IEEE Sensors Journal*, vol. 21, no. 13, pp. 15 012–15 021, 2021.
[26] G. Mao, Y. Zhang, Y. Xu, X. Li, M. Xu, Y. Zhang, and P. Jia, "An electronic nose for harmful gas early detection based on a hybrid deep learning method h-crnn," *Microchemical Journal*, vol. 195, p. 109464, 2023. [Online]. Available: https://www.sciencedirect.com/science/article/pii/S0026265X23010834
[27] D. Aulia, R. Sarno, S. C. Hidayati, and M. Rivai, "Optimization of the Electronic Nose Sensor Array for Asthma Detection Based on Genetic Algorithm," *IEEE Access*, vol. PP, p. 1, 2023.
[28] X. Pan, H. Zhang, W. Ye, A. Bermak, and X. Zhao, "A Fast and Robust Gas Recognition Algorithm Based on Hybrid Convolutional and Recurrent Neural Network," *IEEE Access*, vol. 7, pp. 100 954–100 963, 2019.
[29] H. Zhang, W. Ye, X. Zhao, R. K. Teng, and X. Pan, "A Novel Convolutional Recurrent Neural Network Based Algorithm for Fast Gas Recognition in Electronic Nose System," *2018 IEEE International Conference on Electron Devices and Solid State Circuits, EDSSC 2018*, vol. 1, no. c, pp. 1–2, 2018.
[30] W. Zhang, L. Wang, J. Chen, W. Xiao, and X. Bi, "A novel gas recognition and concentration detection algorithm for artificial olfaction," *IEEE Transactions on Instrumentation and Measurement*, vol. 70, pp. 1–14, 2021.
[31] M. J. Oates, J. D. Gonzalez-Teruel, M. C. Ruiz-Abellon, A. Guillamon-Frutos, J. A. Ramos, and R. Torres-Sanchez, "Using a Low-Cost Components e-Nose for Basic Detection of Different Foodstuffs," *IEEE Sensors Journal*, vol. 22, no. 14, pp. 13 872–13 881, 2022.
[32] M. Modesti, I. Taglieri, A. Bianchi, A. Tonacci, F. Sansone, A. Bellincontro, F. Venturi, and C. Sanmartin, "E-Nose and Olfactory Assessment : Teamwork or a Challenge to the Last Data ? The Case of Virgin Olive Oil Stability and Shelf Life," *Applied Sciences*, vol. 11, p. 8453, 2021.
[33] M. C. Cerrato Oliveros, J. L. Pérez Pavón, C. García Pinto, M. E. Fernández Laespada, B. Moreno Cordero, and M. Forina, "Electronic nose based on metal oxide semiconductor sensors as a fast alternative for the detection of adulteration of virgin olive oils," *Analytica Chimica Acta*, vol. 459, no. 2, pp. 219–228, 2002.
[34] M. R. Zarezadeh, M. Aboonajmi, M. G. Varnamkhasti, and F. Azarikia, "Olive Oil Classification and Fraud Detection Using E-Nose and Ultrasonic System," *Food Analytical Methods*, vol. 14, no. 10, pp. 2199–2210, 2021. [Online]. Available: https://doi.org/10.1007/s12161-021-02035-y
[35] M. J. Lerma-García, E. F. Simó-Alfonso, A. Bendini, and L. Cerretani, "Metal oxide semiconductor sensors for monitoring of oxidative status evolution and sensory analysis of virgin olive oils with different phenolic content," *Food Chemistry*, vol. 117, no. 4, pp. 608–614, 2009. [Online]. Available: http://dx.doi.org/10.1016/j.foodchem.2009.04.052
[36] T. Eklöv, G. Johansson, F. Winquist, and I. Lundström, "Monitoring Sausage Fermentation Using an Electronic Nose," *Journal of the Science of Food and Agriculture*, vol. 76, no. 4, pp. 525–532, 1998.
[37] R. Selvaraj, N. J. Vasa, S. M. Nagendra, and B. Mizaikoff, "Advances in mid-infrared spectroscopy-based sensing techniques for exhaled breath diagnostics," *Molecules*, vol. 25, no. 9, pp. 1–17, 2020.
[38] P. Montuschi, N. Mores, A. Trové, C. Mondino, and P. J. Barnes, "The electronic nose in respiratory medicine," *Respiration*, vol. 85, no. 1, pp. 72–84, 2012.
[39] K. D. van de Kant, L. J. van der Sande, Q. Jöbsis, O. C. van Schayck, and E. Dompeling, "Clinical use of exhaled volatile organic compounds in pulmonary diseases: A systematic review," *Respiratory Research*, vol. 13, 2012.
[40] B. Behera, R. Joshi, G. A. Vishnu, S. Bhalerao, and H. Pandya, "Electronic-nose: A non-invasive technology for breath analysis of diabetes and lung cancer patients," *J. Breath Res. Accept.*, vol. 13, no. 2, 2019.
[41] L. Díaz de León-Martínez, R. Flores-Ramírez, C. M. López-Mendoza, M. Rodríguez-Aguilar, G. Metha, L. Zúñiga-Martínez, O. Ornelas-Rebolledo, and L. E. Alcántara-Quintana, "Identification of volatile organic compounds in the urine of patients with cervical cancer. Test concept for timely screening," *Clinica Chimica Acta*, vol. 522, pp. 132–140, nov 2021. [Online]. Available: https://linkinghub.elsevier.com/retrieve/pii/S0009898121002928
[42] M. Nakıp, O. Çopur, E. Biyik, and C. Güzeliş, "Renewable energy management in smart home environment via forecast embedded scheduling based on recurrent trend predictive neural network," *Applied Energy*, vol. 340, p. 121014, 2023.

This work is licensed under a Creative Commons Attribution-NonCommercial-NoDerivatives 4.0 License. For more information, see https://creativecommons.org/licenses/by-nc-nd/4

This article has been accepted for publication in IEEE Access. This is the author's version which has not been fully edited and content may change prior to final publication. Citation information: DOI 10.1109/ACCESS.2024.3401569

PERVİN BULUCU recevied her B.Sc. and M.Sc. degrees in Electrical-Electronics Engineering from Dokuz Eylül University (Izmir, Turkey) in 2015 and 2019 respectively. She worked on utilizing three dimensional convolutional neural networks for the semantic segmentation of liver Computed tomography angiography images for her M. Sc. thesis. Furthermore, she worked on Nonlinear Autoregressive Moving-average controller on real life and simulated plants for a TUBITAK 1001 project during her masters. Currently, she is a Ph.D. candidate at Yaşar University (Izmir, Turkey) and working on E-Nose systems.

MERT NAKIP obtained his B.Sc. degree, graduating ranked first in his class from the Electrical-Electronics Engineering at Yaşar University (Izmir, Turkey) in 2018. His design of a multi-sensor fire detector via machine learning methods was ranked #1 nationally at the Industry-Focused Undergraduate Graduation Projects Competition organized by TÜBİTAK (Turkish Scientific and Technological Research Council). He completed his M. Sc. thesis in Electrical-Electronics Engineering at Yaşar University (Izmir, Turkey) in 2020. His thesis focused on the application of machine learning methods to IoT and was supported by the National Graduate Scholarship Program of TÜBİTAK 2210C in High-Priority Technological Areas. Currently a Research Assistant and Ph.D. Candidate at the Institute of Theoretical and Applied Informatics, Polish Academy of Sciences (Gliwice, Poland), he is also a researcher in the DOSS project of the European Commission H2020 Program.

CÜNEYT GÜZELİŞ received the B.Sc., M.Sc., and Ph.D. degrees in Electrical Engineering from Istanbul Technical University (Istanbul, Turkey) in 1981, 1984, and 1988, respectively. He was a visiting researcher and lecturer between 1989 and 1991 in the Department of Electrical Engineering and Computer Sciences at the University of California, Berkeley (Berkeley, CA). He served as a full-time faculty member at Istanbul Technical University from 1991 to 2000, where he became full professor in 1998. He was Professor of Electrical and Electronics Engineering at Dokuz Eylül University (İzmir, Turkey) from 2000 to 2011, where he has served as the Dean of the Faculty of Engineering, and at İzmir University of Economics (İzmir, Turkey) from 2011 to 2015, where he has served as the Director of the Graduate School of Natural and Applied Science. Since 2015, he has been Professor of Electrical and Electronics Engineering at Yaşar University (İzmir, Turkey), where he has served as the Director of the Graduate School. He has supervised 17 M.S. and 14 Ph.D. students and published over 50 SCI indexed journal papers, 6 peer-reviewed book chapters, and more than 80 peer-reviewed conference papers. He has participated in over 20 scientific research projects funded by national and international institutions, such as the British Council and the French National Council for Scientific Research. His research interests include artificial neural networks, biomedical signal and image processing, nonlinear circuits-systems and control as well as educational systems.

This work is licensed under a Creative Commons Attribution-NonCommercial-NoDerivatives 4.0 License. For more information, see https://creativecommons.org/licenses/by-nc-nd/4